Shear flow behaviour of bidisperse rod-like

colloids

Christian Lang*,† and Minne Paul Lettinga*,‡,¶

†Jülich Centre for Neutron Science, Forschungszentrum Jülich, Germany ‡Institute for Complex Systems 3, Forschungszentrum Jülich, Germany ¶Laboratory of Soft Matter and Biophysics, KU Leuven, Belgium

E-mail: c.lang@fz-juelich.de; p.lettinga@fz-juelich.de

Abstract

An a priori prediction of the flow properties of polydisperse rod-like macromolecules is a prerequisite for the understanding of many industrial and biological processes. Using mixtures of two naturally monodisperse viruses, we create a benchmark bidisperse suspension of rod-like colloids to test the effect of length bidispersity on the shear flow behaviour. We find that the zero-shear viscosity is a non-linear function of the fraction of long rods, due to the strong length dependence of the rotational dynamics, which determine this quantity. With increasing concentration and fraction of long rods, the shear thinning gets more pronounced, following the predictions of our recently proposed theory which we extended for bidisperse mixtures. This theory allows for a quantitative prediction of the flow properties of bi- and polydisperse mixtures of ideal rods at least for moderate polydispersity.

Introduction

Purely steric interactions between colloidal rods can lead to a huge enhancement of the rheological response of many soft matter systems, already at very moderate concentrations. The most prominent example in biology are filamentous particles like F-actin and microtubuli which give strength to the cytoskeleton. ¹⁻³ There are, however, many more filamentous particles that can be extracted from nature, which strongly affect the rheology, such as viruses, ⁴⁻⁶ polysaccharides, ⁷⁻⁹ fibres from denatured proteins, ¹⁰⁻¹² and cellulose in various forms. ^{13,14} The rod-like systems increasingly find applications, for example as viscosity modifiers in consumer goods, ¹⁵⁻¹⁷ because they are much more efficient to tailor the rheological response than traditional materials. Vice versa, synthetic routes have been explored to produce stiff self-assembled supra-molecular particles ^{18,19} that can form biomimetic hydrogels ²⁰⁻²² and synthetic rod-like systems, such as aramids ²³ and carbon nano-tubes, ²⁴ are the building blocks in the production of strong fibres. ^{25,26}

The main rheological properties of semi-dilute isotropic suspensions of rods, the high zero-shear viscosity and strong shear thinning behaviour, have been partly understood showing qualitative agreement between theoretical predictions $^{27-30}$ and experiments. $^{7,31-34}$ It was established that the rheological response is governed by the rotational diffusion coefficient, D_r . In semi-dilute suspensions of rods, the Doi-Edwards tube model 29 predicts that: $D_r = cD_r^{(0)}(\nu L^3)^{-2}$, where ν is the number density, L the rod length, and $D_r^{(0)} = 3k_BT \ln(L/d)/\pi\eta_s L^3$ is the rotational diffusion coefficient of a single rod 35 at infinite dilution depending additionally on the rod diameter d and the viscosity of the solvent η_s . This leads to a strong length 32 and concentration 9,31 dependence of the zero-shear viscosity: $\eta_0 \sim (\nu L^3)^3$. This theory was further improved, taking into account head-on collisions of rods at high concentrations, 36 and stretching the range of concentrations for which the theory applies. 30 In a recent study, we have shown that the length and concentration dependence of the zero-shear viscosity as well as the shear thinning can be fully described, when the full shear-induced dilation of the confining tubes is taken into account additionally. 37 To this

end, we employed a library of monodisperse filamentous viruses, which we studied using a combination of rheology and small angle neutron scattering.

As most systems introduced above are intrinsically polydisperse in length, experimental studies face the challenge of correctly interpreting the observed flow behaviour. 38-47 Also for the case of entangled polydisperse linear polymers, a number of open questions remain regarding the effect of polydispersity on the flow behaviour. 48,49 Understanding the effect of polydispersity on the flow behaviour is thus essential, for example, to rationally tune the properties of polydisperse industrial rod-like polymer suspensions. For this purpose, Marrucci and Grizzuti^{50,51} (MG) extended the theory of Doi and Edwards, ^{29,52} originally pioneered by Hess²⁸ and later rewritten (exchanging the unknown mean-field potential between rods by excluded volume interactions) by Dhont and Briels.⁵³ MG theory can be subsumed under two main premises: First, the zero-shear viscosity and the shear thinning of rods depend on the rod length, such that longer rods have a higher zero-shear viscosity than shorter ones but achieve better orientational ordering than their short counterparts, leading to a stronger shear thinning behaviour. Second, the fastest diffusion process determines the low shear rate behaviour, since the presence of shorter rods in the mixture speeds up the rotation of the longer rods, but the presence of longer rods does not slow down the shorter rods, ⁵⁴ similar to the relaxation process found in entangled linear bidisperse blends of flexible polymers. 48 This leads to a zero-shear viscosity increasing linearly with the decreasing content of the shorter species. As a result, the short rods dominate over the long ones in the low shear rate regime, while at high shear rates, the longer rods help the orientational ordering of the short species. The second of these assumptions, however, has been disputed by Larson and Mead, ⁵⁴ who demonstrated that the dynamics of both rod species in the quasi-linear deformation regime are equally important, since the longer species slows the rotation of the shorter one down, while the presence of shorter species allows for a relatively faster rotation of the longer one.

In this work, we use our benchmark system of filamentous viruses to demonstrate that

Larson and Mead had the correct idea for modifying the MG theory and we make the suggested changes explicit, using our recently developed extension to finite shear rates. ³⁷ For this purpose, we use suspensions of monodisperse fd virus (L=0.88 μ m, L_p =2.8±0.7 μ m) and pf1 virus (L=1.96 μ m, L_p =2.8±0.7 μ m) and create a controlled length bidispersity by stoichiometric mixing, keeping the overall volume fraction constant. We study the effect of bidispersity on the shear flow behaviour of these suspensions in the semi-dilute concentration regime. While the shear thinning as predicted by the MG theory is correct, our experiments suggest that the zero-shear viscosity is not a linear function of the content of the shorter species. Therefore, we propose a different mixing rule for the rotational diffusivity of the bidisperse system based on Larson and Mead's idea, resulting in a non-linear interdependence of zero-shear viscosity and content of the shorter particles. Together with our recently proposed pre-factor for the rotational diffusion coefficient, ³⁷ we quantitatively predict the complete shear flow behaviour of the bidisperse mixtures.

The paper is structured as follows: First, the Marrucci-Grizzuti and the Larson-Mead theories are described and integrated with our recently improved theory for sheared rods. Then, we compare our theoretical results to the rheological data in the linear visco-elastic and non-linear shear thinning regime. Finally, we discuss the results.

Theory

We start the theory section by revisiting the theory for dispersions of monodisperse rods, which we recently extended to describe the zero-shear viscosity as well as the shear thinning behaviour as a function of concentration and length.³⁷ We will then implement this theory in the original Marrucci and Grizzuti (MG) theory ^{50,51} and the more recent approach by Larson and Mead (LM).⁵⁴

From the full Yvon-Born-Green (YBG) hierarchy^{55,56} of Smoluchowski equations⁵⁷ for rigid large aspect-ratio rods, Dhont and Briels⁵³ derived an equation of motion for the

orientational ordering tensor **S** of rods subject to a velocity gradient Γ :

$$\frac{d\mathbf{S}}{dt} = -6D_r^{(0)} \left[\mathbf{S} - \frac{1}{3} \mathbf{I} + \frac{\pi}{4} \nu dL^2 \left(\mathbf{S}^{(4)} : \mathbf{S} - \mathbf{S} \cdot \mathbf{S} \right) \right]
+ \mathbf{\Gamma} \cdot \mathbf{S} + \mathbf{S} \cdot \mathbf{\Gamma}^T - 2\mathbf{S}^{(4)} : \mathbf{E} ,$$
(1)

where **I** is the unit tensor, d the thickness of the rods, and **E** is the rate of strain tensor. The pre-requisites for their result are an equilibrium pair-correlation function (based on the Maier-Saupe potential), truncated at the pair level, 57,58 and a constant rotational diffusion coefficient, $D_r^{(0)}$. Equation 1 is analytically solvable by using the closure relation:

$$\mathbf{S}^{(4)}: \mathbf{A} = \frac{1}{5} [\mathbf{S} \cdot \overline{\mathbf{A}} + \overline{\mathbf{A}} \cdot \mathbf{S}^T - \mathbf{S} \cdot \mathbf{S} \cdot \overline{\mathbf{A}} - \overline{\mathbf{A}} \cdot \mathbf{S} \cdot \mathbf{S} + 2\mathbf{S} \cdot \overline{\mathbf{A}} \cdot \mathbf{S} + 3\mathbf{S}\mathbf{S} : \overline{\mathbf{A}}]$$
(2)

for the fourth order alignment tensor $S^{(4)}$, where \overline{A} can be any symmetrical tensor. Together with their expression for the stress tensor of the liquid,

$$\Sigma = 2\eta_s \mathbf{E} + 3\nu k_B T [\mathbf{S} - \frac{1}{3}\mathbf{I} + \frac{\pi}{4}\nu dL^2 \left(\mathbf{S}^{(4)} : \mathbf{S} - \mathbf{S} \cdot \mathbf{S} \right)$$

$$+ \frac{1}{6D_r^{(0)}} \left(\mathbf{S}^{(4)} : \mathbf{E} - \frac{1}{3}\mathbf{I}\mathbf{S} : \mathbf{E} \right)] , \qquad (3)$$

where η_s is the solvent viscosity, and k_BT is the thermal energy, all visco-elastic response functions of a rod-like suspension can be calculated from the molecules orientational behaviour under flow.

We extended this theoretical framework, based on our earlier experimental investigations on quasi-ideal suspensions of rod-like colloids.^{37,59} Since the YBG hierarchy is truncated at the pair-level and the pair-correlation function is flow independent, equation 1 does not correctly predict the zero-shear viscosity and the strong shear thinning behaviour of semi-dilute suspensions of rods. Therefore, we include both effects into the definition of an effective rotational diffusion coefficient, interpolating between the pre-averaged rotational

diffusion coefficient introduced by Doi and Edwards, ²⁹ which we expanded in terms of S, and $D_r^{(0)}$:

$$D_r^{\text{eff}} = \frac{D_r^{(0)}}{1 + \frac{1}{c} \left[\frac{5}{4} \nu L^3 \left(1 - \frac{3}{5} \mathbf{S} : \mathbf{S} - \frac{2}{5} \left(\mathbf{S} : \mathbf{S} \right)^2 \right) \right]^2} , \tag{4}$$

where we have experimentally determined 37 the pre-factor $c = 1.1 \times 10^3$. Using this expression instead of $D_r^{(0)}$ in equation 1, we achieve a correct diffusion coefficient for low and high concentrations and further incorporate a full dilation of the tube at high shear rates. For both high shear rates and low concentrations in terms of number densities, we thus find $D_r^{\text{eff}} \to D_r^{(0)}$. At high shear rates, this limiting value assures a substantial increase in the rotational motility of the particles that allows for the strong shear thinning we observe experimentally.

We extend this theory to bidisperse mixtures of rods first by employing the Marrucci-Grizzuti (MG) extension.^{50,51} We can determine the number density, $\nu^{(m)}$, of the mixture by the following linear mixing rule:

$$\nu^{(m)} = \rho \nu_1 + (\rho - 1)\nu_2 \quad , \tag{5}$$

where ρ is called the mixing parameter from now on. For both of the $i = \{1, 2\}$ species in the mixture, with lengths L_i and number densities ν_i , we can write the equation of motion for their individual ordering tensors, \mathbf{S}_i , as follows:

$$\frac{d\mathbf{S}_{i}}{dt} = -6D_{r,i}^{\text{eff}} \left[\mathbf{S}_{i} - \frac{1}{3}\mathbf{I} + \frac{\pi}{4}dL_{i} \sum_{j=1}^{2} \nu_{j} L_{j} \left(\mathbf{S}_{i}^{(4)} : \mathbf{S}_{j} - \mathbf{S}_{j} \cdot \mathbf{S}_{i} \right) \right] + \mathbf{\Gamma} \cdot \mathbf{S}_{i} + \mathbf{S}_{i} \cdot \mathbf{\Gamma}^{T} - 2\mathbf{S}_{i}^{(4)} : \mathbf{E} .$$
(6)

Accordingly, the stress tensor becomes:

$$\Sigma = 2\eta_s \mathbf{E} + 3k_B T \sum_{i=1}^{2} \nu_i [\mathbf{S}_i - \frac{1}{3} \mathbf{I}$$

$$+ \frac{\pi}{4} dL_i \sum_{j=1}^{2} \nu_j L_j \left(\mathbf{S}_i^{(4)} : \mathbf{S}_j - \mathbf{S}_j \cdot \mathbf{S}_i \right)$$

$$+ \frac{1}{6D_{r,i}^{(0)}} \left(\mathbf{S}_i^{(4)} : \mathbf{E} - \frac{1}{3} \mathbf{I} \mathbf{S}_i : \mathbf{E} \right)] .$$

$$(7)$$

The effective rotational diffusion coefficients of both species in the MG framework read:

$$D_{r,i}^{\text{eff}} = \frac{D_{r,i}^{(0)}}{1 + \frac{1}{c}f} \quad , \tag{8}$$

with the MG mixing rule:

$$f = L_i \left[\frac{5}{4} \sum_{j=1}^2 \nu_j L_j \left(1 - \frac{3}{5} \mathbf{S}_i : \mathbf{S}_j \right) \right] \times$$

$$\times \left[\frac{5}{4} \sum_{j \le i} \nu_j L_j^4 \left(1 - \frac{3}{5} \mathbf{S}_i : \mathbf{S}_j \right) \right]$$

$$+ \frac{5}{4} L_i^4 \sum_{j > i} \nu_j L_j \left(1 - \frac{3}{5} \mathbf{S}_i : \mathbf{S}_j \right) \right] , \qquad (9)$$

based on the assumption that the short species dominates over the long one.

We also extend our theory by applying the suggestion of Larson and Mead (LM),⁵⁴ where it is the average length of the rods in the mixture that determines both the tube size as well as the diffusivity of the rods. In this case, we propose the following effective rotational diffusion coefficient instead of equation 8:

$$D_{r,i}^{\text{eff}} = \frac{D_{r,i}^{(0)}}{1 + \frac{1}{c} \left[\frac{5}{4} \sum_{j=1}^{2} \nu_j L_j^3 \left(1 - \frac{3}{5} \mathbf{S}_i : \mathbf{S}_j - \frac{2}{5} \left(\mathbf{S}_i : \mathbf{S}_j \right)^2 \right) \right]^2} , \tag{10}$$

where $D_{r,i}^{(0)} = 3k_BT \ln \left(L_i/d\right)/\pi \eta_s L_i^3$. So, we essentially assume that both species are equally

important. In equilibrium, the second term in the denominator simplifies to:

$$\frac{1}{c} \left[\sum_{j=1}^{2} \nu_j L_j^3 \right]^2 \quad . \tag{11}$$

Together, equations 6, 7, and 10 build a theoretical framework which allows for a numerical calculation of the visco-elastic material functions of length-bidisperse mixtures of rigid rods and their orientational ordering under flow, characterized by the largest eigenvalue of the orientational ordering tensor of the whole system, λ_1 , or the orientational order parameter, $\langle P_2 \rangle = (3\lambda_1 - 1)/2$. Here, we focus on the simple shear flow behaviour of semi-dilute suspensions, for which the velocity gradient tensor and the rate of strain tensor are well-known and the orientational closure relation, equation 2, holds.^{53,60}

FIG. 1 shows two model calculations of the viscosity, η , and orientational order parameter, $\langle P_2 \rangle$, as a function of the shear rate, $\dot{\gamma}$, for $\varphi = 5.4 \text{x} 10^{-3}$, $T = 25^{\circ}C$, $\eta_s = 8.9 \text{x} 10^{-4}$, and d = 10.5 nm for length-bidisperse mixtures of $L = 1.96 \ \mu\text{m}$ (black) and $L = 0.88 \ \mu\text{m}$ (light grey). The depicted curves correspond to mixing parameters of $\rho = \{0, 0.1, 0.3, 0.5, 0.7, 0.9, 1\}$, shaded from light grey for $\rho = 0$ to black for $\rho = 1$. The result in FIG. 1(a) illustrates the mixing of ordering and viscosity according to MG theory, using equations 6, 7, and 8. The result in FIG. 1(b) shows the outcome of the approach suggested by Larson and Mead, combining equations 6, 7, and 10.

Whilst the orientational ordering (dotted lines in FIG 1) smoothly changes for the LM theory, the MG theory predicts a pronounced bimodal ordering for intermediate mixing parameters with an inflection point of the curve located around a shear rate of 3 s^{-1} , roughly corresponding to the bare Péclet number, $Pe^{(0)} = \dot{\gamma}/D_r^{(0)} = 1$, for the long species. In the MG theory, this marks the shear rate, at which the long species is fully oriented and dominates the rheological behaviour, as indicated by the curves for $\langle P_2 \rangle$ of the long (red) and short (blue) species which results in the purple bimodal curve in FIG 1(a). Further, comparing the ordering of the long species alone (black dotted) to its ordering in presence of 50% of

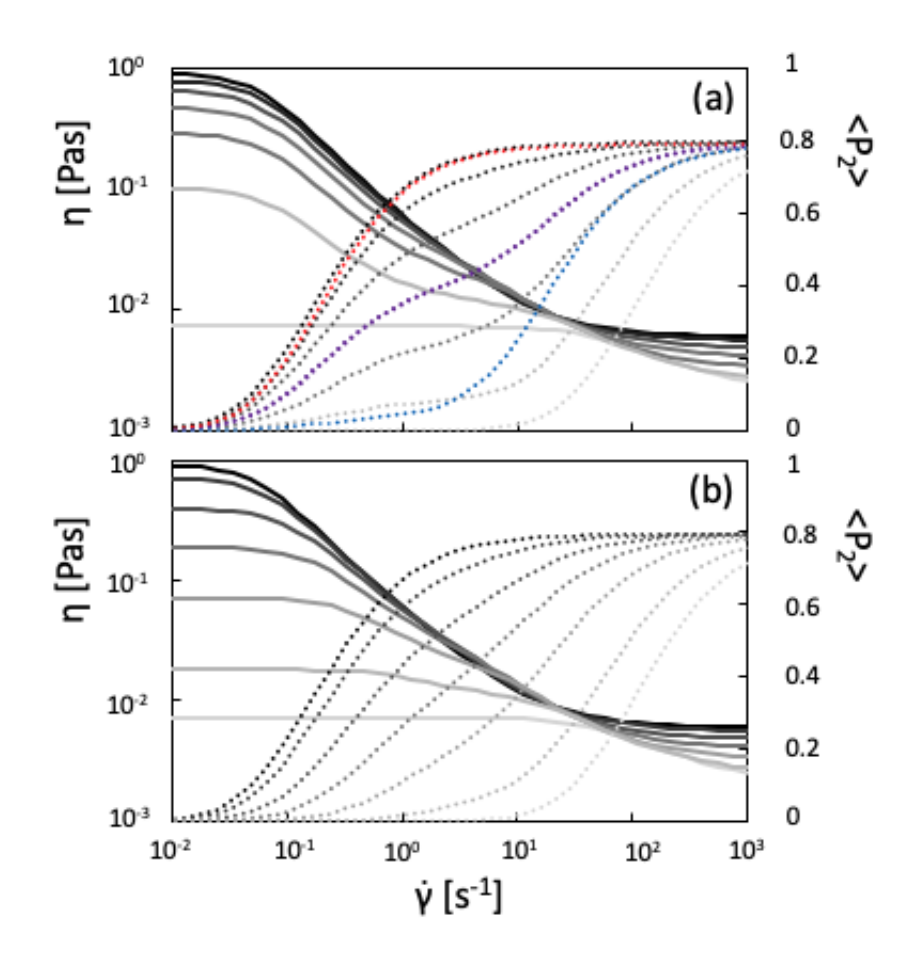


Figure 1: Viscosity (full lines) and orientational order parameter (dotted lines) from (a) MG theory and (b) the new theory for bidisperse mixtures of rods at $\varphi = 5.4 \text{x} 10^{-3}$, following LM, with varying content of the long particle, shaded from 100% long (black) to 0% long, or 100% short (light grey). The purple ordering in (a) for $\rho = 0.5$ results from the ordering of the long species (red) and the short species (blue).

the short species (red dotted), and the ordering of the short species alone (pale grey dotted) to its ordering in the presence of 50% of the long species (blue dotted), we can clearly see the predicted dominance of the long species over the short one at intermediate to high shear rates.

Accordingly, the viscosity curves (full lines in FIG. 1) in the MG theory for intermediate mixing parameter have a bimodal shape resulting from the inflection in the orientational ordering. Additionally, we find a zero-shear viscosity, increasing linearly with the mixing parameter, and, therefore, also with the increasing content of the long species.

In contrast, the LM based theory, shown in FIG. 1(b), neither predicts inflection points

of orientational ordering, nor of the viscosity curves. Additionally, the zero-shear viscosity is a non-linear function of the content of the long species.

Experiments and Materials

Experiments

For our experimental investigation, we used a strain-controlled ARES LS rheometer (TA Instruments, Newcastle, USA) equipped with a single wall Couette cell of 1 mm gap width. After loading the sample, we applied 1 min of pre-shear at 100 s^{-1} , and waited for 10 min for orientational equilibration, to erase possible effects from sample loading. We conducted step rate tests at constant shear rates in the range $\dot{\gamma} \in [0.001, 1000] s^{-1}$, measuring the shear stress, Σ_{21} , as a function of time, see FIG. 2. After an initial re-orientation process of the rods, marked by an overshoot of Σ_{21} with an amplitude depending on the shear rate, the stress remains constant. We calculate the sample viscosity, $\eta = \Sigma_{21}/\dot{\gamma}$, for every shear rate in the indicated range from a time averaged value of Σ_{21} in this constant regime.

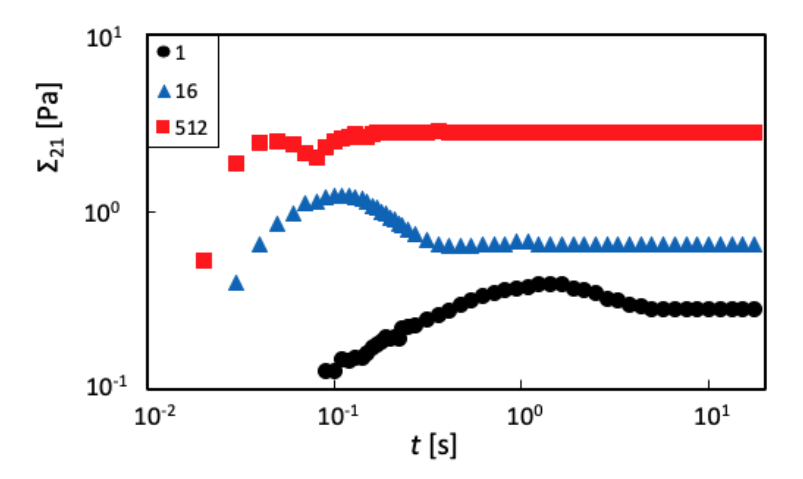


Figure 2: Shear stress as a function of time for Pf1 virus (L=1.96 μ m, $L_p = 2.9 \pm 0.7 \mu$ m) at a concentration of 6.8 mg/ml for three different shear rates: $\dot{\gamma} = 1, 16, 512 \ s^{-1}$.

Materials

Fd virus was amplified in an infected XL-1 blue bacteria strain of Escherichia coli, nourished from Luria-Bertani broth, 61,62 following a standard biological protocol. 63 Pf1 virus was purchased from ASLA Biotech, Riga, Latvia. After purification by ultra-centrifugation, both species were suspended in Trizma buffer, adjusted to pH 8.3, containing deionized water with 20 mM/l Trizma base and 90 mM/l NaCl, amounting to an ionic strength of 100 mM. At this ionic strength, the effective diameter of our rods is 10.5 nm, including the Debye double layer. 64 Both suspensions were concentrated to the nematic liquid crystalline state and subsequently diluted to their isotropic binodal points, $L\varphi_I/d_{\text{eff}} = 4.61$ for fd and $L\varphi_I/d_{\text{eff}} = 8.37$ for Pf1, comparing well to the theoretical prediction by Chen. 65 This confirms their different contour lengths of $L = 0.88 \ \mu\text{m}$ for fd and $L = 1.96 \ \mu\text{m}$ for Pf1. The persistence length of both species is $2.8\pm0.7 \ \mu\text{m}$. 66

From the nematic stock suspensions, we produced two semi-dilute suspensions of 2.3 and 6.8 mg/ml. At these constant volume fractions, we mixed the two species according to the mixing rule $\nu^{(m)} = \rho \nu^{(\text{pf1})} + (\rho - 1)\nu^{(\text{fd})}$, where ν is the number density of the rods.

Results and Discussion

The non-linear viscosity of bidisperse mixtures of rods in the semi-dilute concentration regime, obtained from the steady-state shear stress values, see FIG. 2, is shown as a function of shear rate in FIG. 3 for constant weight fractions of (a) 2.3 mg/ml and (b) 6.8 mg/ml. The mixing parameters are $\rho = \{0, 0.1, 0.3, 0.5, 0.7, 0.9, 1\}$ for the low concentration and $\rho = \{0, 0.1, 0.3, 0.5, 0.7, 0.8, 1\}$ for the high concentration, shaded from black, 100% $L = 1.96 \ \mu \text{m}$ to light grey, 100% $L = 0.88 \ \mu \text{m}$.

We employ the Carreau equation ⁶⁷ as a fitting function, shown as lines in FIG 3,

$$\eta = \eta_s + (\eta_0 - \eta_s)/(1 + A\dot{\gamma}^2)^B \quad , \tag{12}$$

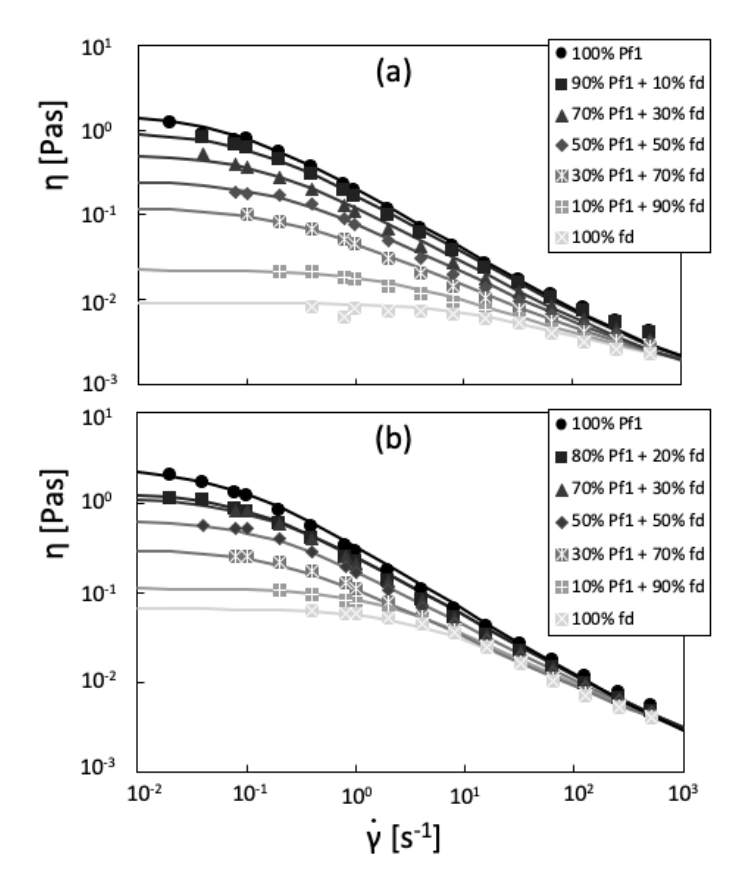


Figure 3: Shear viscosity as a function of shear rate for (a) 2.4 mg/ml and (b) 6.8 mg/ml of bidisperse mixtures of Pf1 (L=1.96 μ m, $L_p = 2.9 \pm 0.7 \mu$ m) and fd (L=0.88 μ m, $L_p = 2.9 \pm 0.7 \mu$ m). The lines are Carreau fits with parameters η_0 , and B shown in FIG. 4 and $A = \{14, 10, 7, 5.5, 5, 0.6, 0.1\}$ sec. in (a) and $A = \{14, 10, 8.5, 7, 5, 0.6, 0.3\}$ sec. in (b) ordered from black (100% long) to light grey (100% short).

with fit parameters η_0 , A, and B, in order to obtain the zero-shear viscosities, η_0 , and shear thinning parameters, B, as a function of the mixing parameter, ρ , see FIG. 4.

We compare the numbers for η_0 and B, obtained from fitting, to the two different theoretical approaches: the MG theory, combining equations 6, 7, and 8, and the LM based theory, combining equations 6, 7, and 10, for (a) $\varphi = 5.4 \times 10^{-3}$, and (b) $\varphi = 1.78 \times 10^{-2}$, with $T = 25^{\circ}C$, $\eta_s = 8.9 \times 10^{-4}$, and d = 10.5 nm for length-bidisperse mixtures of $L = 1.96 \ \mu \text{m}$ (dark symbols) and $L = 0.88 \ \mu \text{m}$ (light symbols). As FIG. 4 indicates, the suspensions at both concentrations show an increase in zero-shear viscosity as well as in the shear thinning parameter with increasing mixing parameter, ρ , which is proportional to the content of the

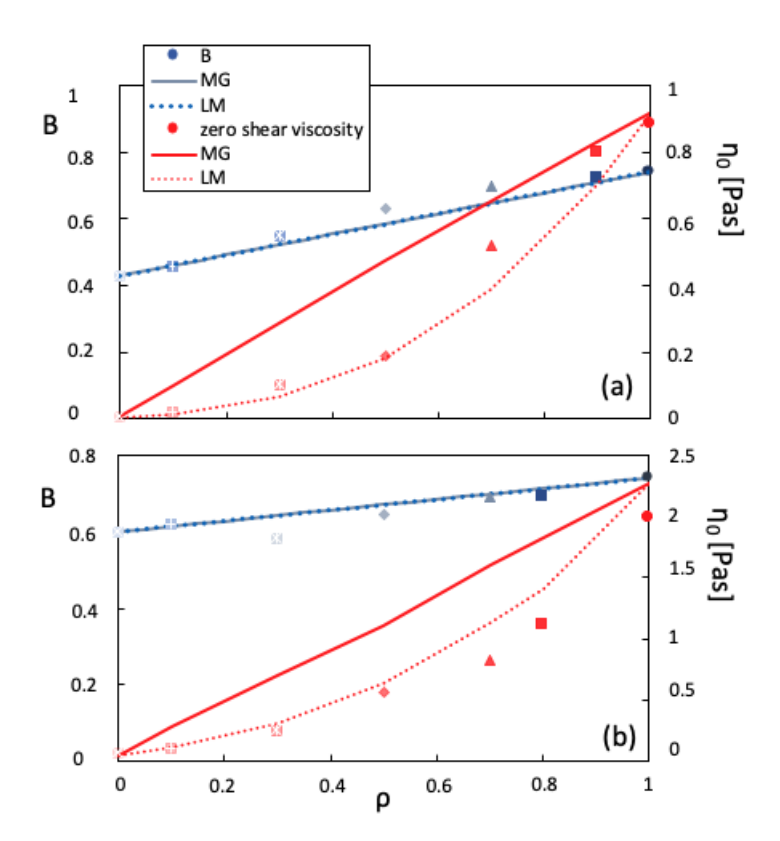


Figure 4: Shear thinning parameter (blue) and zero-shear viscosity (red) as a function of the mixing parameter obtained from the Carreau fits in FIG. 3 for (a) 2.4 mg/ml and (b) 6.8 mg/ml. Full lines show the MG theory, dotted lines the LM theory. The theoretical B values are mean values between $\dot{\gamma} = 0.1$ and $\dot{\gamma} = 100$, except for 100% fd, where the mean value is taken between $\dot{\gamma} = 50$ and $\dot{\gamma} = 200$.

long particle, Pf1. We observe that the shear thinning parameter increases more or less linearly with the mixing parameter, while the increase of the zero-shear viscosity is clearly non-linear. As mentioned above, the MG theory predicts a linear increase of both quantities with increasing content of the long species (or decreasing content of the short species) in the bidisperse mixture. This results from a dominance of the short species over the long one in terms of the rotational diffusion coefficient, as observed for flexible polymers. ⁴⁸ In the LM based approach, both species contribute evenly to the hindrance of rotation. This results in a non-linear increase of the zero-shear viscosity with the content of the longer particle, but since the longer particle dominates the shear thinning behaviour, see FIG 1(a), the mean shear thinning parameter scales linearly with the mixing parameter and therefore depends

mainly on the content of the long species. Though the LM based theory treats both species as equally important, it is indeed the long species which governs the shear thinning behaviour at higher shear rates corresponding to bare Péclet numbers above $Pe^{(0)} = \dot{\gamma}/D_r^{(0)} = 1$ for the long species. Thus, the prediction by MG theory equals the prediction of the LM based approach for the shear thinning parameter. Therefore, both approaches are in good agreement with the effect of shear thinning we measure in our systems.

The zero-shear viscosity of bidisperse mixtures of particles with aspect ratios as high as 83.8 and 186.7, on the contrary, is only captured by the LM approach. This stands in marked contrast to the reported behaviour of entangled bidisperse linear polymer blends, where the relaxation time of the longer species is significantly changed by the presence of the shorter species but not vice versa. 48 We remark that the MG theory is likely still correct for the case of bidisperse mixtures of two species with very different aspect ratios. If the aspect ratio of the long particles is much higher than that of the short particles, the particle dynamics of the mixture most likely would scale linearly with the content of the long particles. We would expect that for a mixture where one species is smaller than the mesh size of the network formed by the other species, MG theory applies, since for such a system, the smaller rods cannot effectively entangle with the larger ones. For the systems tested here, with volume fractions of $\varphi = 5.4 \times 10^{-3}$, and 1.78×10^{-2} , far above the overlap concentration, we can estimate the equilibrium mesh size, $\xi = d(\frac{2}{3}\varphi)^{-0.5}$, to be 175 nm, and 96 nm. With a length of the smaller particles of 880 nm, this threshold is clearly exceeded, such that both species effectively entangle with one another in the low shear rate regime. It remains to be tested whether there exists such a threshold for the difference between the aspect ratios, above which our theory for the rotational diffusivity crosses over to the MG theory. With our experimental systems at hand, such a test is not feasible.

Finally, we plot the viscosity curves of the LM based theory together with our experimental results in FIG. 5 in order to test if the functional shape of the curve is correct.

We find a good agreement between theory and experiment for all mixtures over a large

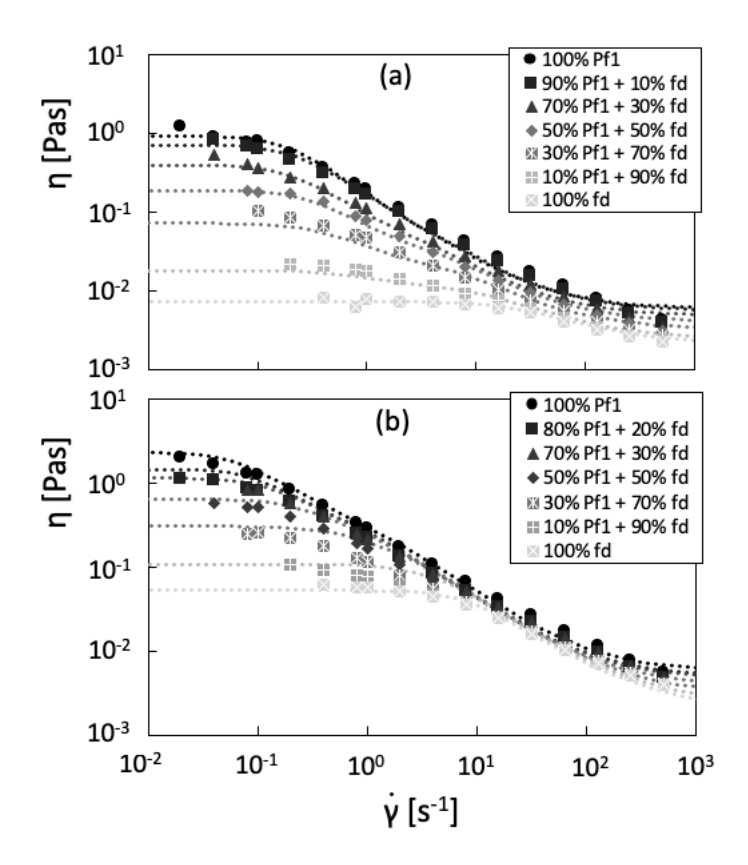


Figure 5: Viscosity as a function of shear rate for (a) 2.4 mg/ml, and (b) 6.8 mg/ml for bidisperse mixtures of (black) Pf1 (L=1.96 μ m, $L_p = 2.9 \pm 0.7 \mu$ m) and (light grey) fd (L=0.88 μ m, $L_p = 2.9 \pm 0.7 \mu$ m). The lines are predictions from the new theory.

shear rate range. At very high shear rates, we observe a minor disagreement between our predictions for the viscosity and the experimental results for higher content of the long species in the case of the lower concentration, shown in FIG. 5(a). This could be due to the effect of flexibility especially of Pf1, as we discussed earlier.³⁷ Neither of the viscosity curves at intermediate mixing parameter display a clear bimodality, and the zero-shear viscosities scale clearly non-linearly with the content of the long particle, as predicted by our proposed theory. This is an indication that it is indeed the average length of particles in the mixture that dictates the low shear rate viscosity, while above a certain shear rate, coinciding with the bare Péclet number, $Pe^{(0)} = \dot{\gamma}/D_r^{(0)} = 1$, of the long particles, the viscosity of the mixture is governed by the alignment of the longer rods as a function of shear rate. At very high shear rates, the particles seem to shear thin slightly more than we predicted, resulting in a

decreasing viscosity over the entire measurable shear rate range. For this reason, we propose the following picture for bidisperse rods of high aspect ratios: At very low shear rates, the particle dynamics are quenched according to the tube model by Doi and Edwards.²⁹ The polydispersity of both the tubes and the rods leads to an averaging effect of the governing dynamics, determining the visco-elastic behaviour such that both species hinder each other in exactly the same fashion, as suggested by Larson and Mead. 54 and it is only the average length of the particles in the mixture which dictates the observable behaviour. At intermediate shear rates, the picture by Marrucci and Grizzuti^{51,51} seems to be correct and it is the longer particles in the bidisperse mixture that govern the shear thinning behaviour due to their relatively high sensitivity to the applied flow field as compared to the shorter rods. At very high shear rates, the influence of hydrodynamics cannot be ignored, as emphasized by Marrucci and Grizzuti. 51 At high Péclet numbers, the theories both predict a length-dependent finite plateau value of the shear viscosity, qualitatively agreeing with the experimental results of Bricker et al. 68 Due to limitations of the used Couette geometry, we could not detect the anticipated high shear rate plateau, and the observed shear thinning continues above shear rates, where the theory predicts the final plateau to occur. Despite these minor difficulties, we conclude that the Dhont-Briels⁵³ stress tensor, modified for bidisperse systems, equation 7, describes the observed rheological response well. These results can thus be used to predict the flow response of polydisperse systems, which are of large importance in industrial applications and biological processes, by taking the actual length distribution of particles into account and accordingly expanding the summation in equations 6, 7, and 10 to i = [1, N] components.

Conclusions

We conclude from our experimental investigation of two constant volume fraction bidisperse mixtures of high aspect ratio rods that the rheological response of these mixtures is not determined by the dynamics or alignment of the shorter species alone, as suggested by Marrucci-Grizzuti theory. Instead, it is the average particle length in the mixture that governs the observable behaviour, as suggested by Larson and Mead. We combined this latter mixing rule with our recently extended theory for rods in shear flow in the semi-dilute concentration regime, employing the experimentally determined pre-factor for the rotational diffusivity, to predict the zero-shear viscosities as well as the shear thinning. The quantitative correspondence between the calculated and measured zero-shear viscosity and shear thinning over a very broad range of shear rates for all compositions of short and long rods confirms the suggested approach. Our findings, thus, point towards a rational prediction of the flow behaviour of polydisperse rod-like systems. The proposed mixing rule is expected to hold for many of the aforementioned bi- and polydisperse rod-like systems with high aspect ratios, concentrations far above the overlap concentration, and moderate polydispersity. In the case of very different aspect ratios, i. e., in a system with very broad polydispersity, we remark that the mixing rule of the original MG theory is likely still correct, as the hindrance of rotation of the long species should cease to affect the very short particles when their contour length becomes small compared to the mesh size of the entanglements formed by the large species.

Acknowledgement

The authors would like to acknowledge Jan Dhont for the stimulating discussions and his help in deriving eq. 4. This research is funded by the European Union within the Horizon 2020 project under the DiStruc Marie Skłodowska Curie innovative training network; grant agreement no. 641839.

References

- Janmey, P. A.; Euteneuer, U.; Traub, P.; Schliwa, M. Viscoelastic Properties of Vimentin Compared with Other Filamentous Biopolymer Networks. J. Cell Biol. 1991, 113, 155–160.
- (2) Isambert, H.; Maggs, A. C. Dynamics and Rheology of Actin Solutions. *Macromolecules* 1996, 29, 1036–1040.
- (3) Semmrich, C.; Storz, T.; Glaser, J.; Merkel, R.; Bausch, A. R.; Kroy, K. Glass transition and rheological redundancy in F-actin solutions. *P. Natl. Acad. Sci. USA* **2007**, *104*, 20199–20203.
- (4) Lauffer, M. A.; Stanley, W. M. Stream double refraction of virus proteins. *J. Biol. Chem.* **1938**, *123*, 507–525.
- (5) Graf, C.; Kramer, H.; Deggelmann, M.; Hagenbuechle, M.; Johner, C.; Martin, C.; Weber, R. Rheological properties of suspensions of interacting rodlike FD-virus particles. J. Chem. Phys. 1993, 98, 4921–4928.
- (6) Schmidt, F. G.; Hinner, B.; Sackmann, E.; Tang, J. X. Viscoelastic properties of semi-flexible filamentous bacteriophage fd. *Phys. Rev. E* **2000**, *62*, 5509–5517.
- (7) Hermans, J. The viscosity of concentrated solutions of rigid rodlike molecules (poly- γ -benzyl-l-glutamate in m-cresol). J. Colloid Sci. 1962, 17, 638–648.
- (8) Tang, H.; Kochetkova, T.; Kriegs, H.; Dhont, J. K. G.; Lettinga, M. P. Shear-banding in entangled xanthan solutions: tunable transition from sharp to broad shear-band interfaces. *Soft Matter* **2018**, *14*, 826–836.
- (9) Takada, Y.; Sato, T.; Teramoto, A. Dynamics of stiff-chain polymers in isotropic solution. 2. Viscosity of aqueous solutions of xanthan, a rigid double-helical polysaccharide. *Macromolecules* 1991, 24, 6215–6219.

- (10) Loveday, S. M.; Wang, X. L.; Rao, M. A.; Anema, S. G.; Singh, H. Beta-Lactoglobulin nanofibrils: Effect of temperature on fibril formation kinetics, fibril morphology and the rheological properties of fibril dispersions. *Food Hydrocolloid.* **2012**, *27*, 242–249.
- (11) Rogers, S. S.; Venema, P.; Sagis, L. M. C.; van der Linden, E.; Donald, A. M. Measuring the length distribution of a fibril system: A flow birefringence technique applied to amyloid fibrils. *Macromolecules* **2005**, *38*, 2948–2958.
- (12) Bolder, S. G.; Sagis, L. M. C.; Venema, P.; van der Linden, E. Effect of stirring and seeding on whey protein fibril formation. *J. Agr. Food Chem.* **2007**, *55*, 5661–5669.
- (13) Urena-Benavides, E. E.; Ao, G. Y.; Davis, V. A.; Kitchens, C. L. Rheology and Phase Behavior of Lyotropic Cellulose Nanocrystal Suspensions. *Macromolecules* 2011, 44, 8990–8998.
- (14) Bercea, M.; Navard, P. Shear Dynamics of Aqueous Suspensions of Cellulose Whiskers. *Macromolecules* **2000**, *33*, 6011–6016.
- (15) Dickinson, E. Colloids in Food: Ingredients, Structure, and Stability. *Annu. Rev. Food Sci. T.* **2015**, *6*, 211–233.
- (16) Nicolai, T.; Britten, M.; Schmitt, C. Beta-Lactoglobulin and WPI aggregates: Formation, structure and applications. *Food Hydrocolloid*. **2011**, *25*, 1945–1962.
- (17) Akkermans, C.; van der Goot, A. J.; Venema, P.; van der Linden, E.; Boom, R. M. Formation of fibrillar whey protein aggregates: Influence of heat and shear treatment, and resulting rheology. *Food Hydrocolloid.* **2008**, *22*, 1315–1325.
- (18) Zhang, J.; Lettinga, P. M.; Dhont, J. K. G.; Stiakakis, E. Direct Visualization of Conformation and Dense Packing of DNA-Based Soft Colloids. *Phys. Rev. Lett.* **2014**, *113*.

- (19) Knoben, W.; Besseling, N. A. M.; Stuart, M. A. C. Rheology of a reversible supramolecular polymer studied by comparison of the effects of temperature and chain stoppers. J. Chem. Phys. 2007, 126.
- (20) Kouwer, P. H. J.; Koepf, M.; Le Sage, V. A. A.; Jaspers, M.; van Buul, A. M.; Eksteen-Akeroyd, Z. H.; Woltinge, T.; Schwartz, E.; Kitto, H. J.; Hoogenboom, R.; Picken, S. J.; Nolte, R. J. M.; Mendes, E.; Rowan, A. E. Responsive biomimetic networks from polyisocyanopeptide hydrogels. *Nature* **2013**, *493*, 651–655.
- (21) Jaspers, M.; Dennison, M.; Mabesoone, M. F. J.; MacKintosh, F. C.; Rowan, A. E.; Kouwer, P. H. J. Ultra-responsive soft matter from strain-stiffening hydrogels. *Nature Comm.* 2014, 5.
- (22) Lovett, J. R.; Derry, M. J.; Yang, P. C.; Hatton, F. L.; Warren, N. J.; Fowler, P. W.; Armes, S. P. Can percolation theory explain the gelation behavior of diblock copolymer worms? Chem. Sci. 2018, 9, 7138–7144.
- (23) Picken, S. J.; Aerts, J.; Visser, R.; Northolt, M. G. Structure and rheology of Aramid solutions: X-ray scattering measurements. *Macromolecules* **1990**, *23*, 3849–3854.
- (24) Fan, Z. H.; Advani, S. G. Rheology of multiwall carbon nanotube suspensions. *J. Rheol.* **2007**, *51*, 585–604.
- (25) Monteiro, S. N.; Lima, E. P.; Louro, L. H. L.; Da Silva, L. C.; Drelich, J. W. Unlocking Function of Aramid Fibers in Multilayered Ballistic Armor. *Metall. Mater. Trans. A* 2015, 46, 37–40.
- (26) Vigolo, B.; Penicaud, A.; Coulon, C.; Sauder, C.; Pailler, R.; Journet, C.; Bernier, P.; Poulin, P. Macroscopic fibers and ribbons of oriented carbon nanotubes. *Science* 2000, 290, 1331–1334.

- (27) Kirkwood, J. G.; Auer, P. L. The visco-elastic properties of solutions of rodlike macro-molecules. *J. Chem. Phys.* **1951**, *19*, 281–283.
- (28) Hess, S. Fokker-Planck-equation approach to flow alignment in liquid crystals. *Z. Natur-forsch.* **1976**, *71*, 1034–1037.
- (29) Doi, M.; Edwards, S. F. Dynamics of rodlike macromolecules in concentrated solution: Part 2. J. Chem. Soc. Faraday Trans. 1978, 74, 918–932.
- (30) Sato, T.; Teramoto, A. Concentrated solutions of liquid-crystalline polymers. *Macro-molecules* **1991**, *24*, 193–196.
- (31) Petekidis, G.; Vlassopoulos, D.; Fytas, G.; Fleischer, G.; Wegner, G. Dynamics of wormlike polymers in solution: Self-diffusion and zero shear viscosity. *Macromolecules* **2000**, *33*, 9630–9640.
- (32) Wierenga, A. M.; Philipse, A. Low-shear viscosity of isotropic dispersions of (Brownian) rods and fibres; a review of theory and experiments. *Colloid. Surface. A* **1998**, *137*, 355–372.
- (33) Fry, M. A.; Langhorst, B.; Kim, H.; Becker, M. L.; Bauer, B. J.; Grulke, E. A.; Hobbie, E. K. Rheo-optical studies of carbon nanotube suspensions. *J. Chem. Phys.* **2006**, 124, 054703.
- (34) Ohshima, A.; Yamagata, A.; Sato, T.; Teramoto, A. Entanglement effects in semiflexible polymer solutions. 3. Zero-shear viscosity and mutual diffusion coefficient of poly(n-hexyl isocyanate) solutions. *Macromolecules* **1999**, *32*, 8645–8654.
- (35) Broersma, S. Rotational diffusion constant of a cylindrical particle. *J. Chem. Phys.* **1960**, *32*, 1626–1632.
- (36) Edwards, S. F.; Evans, K. E. Dynamics of Highly Entangled Rod-like Molecules. *J. Chem. Soc. Faraday Trans.* **1982**, *78*, 113–121.

- (37) Lang, C.; Radulescu, A.; Kohlbrecher, J.; Porcar, L.; Sellinghoff, K.; Dhont, J. K. G.; Lettinga, M. P. Microstructural understanding of the length and stiffness dependent shear thinning in semi-dilute colloidal rods. *Macromolecules* **2019**, *52*, 9604–9612.
- (38) Maschmeyer, R. O.; Hill, C. T. Rheology of concentrated suspensions of fibers in tube flow. II. An Exploratory Study. *Trans. Soc. Rheol.* **1977**, *21*, 183–194.
- (39) Chu, S. G.; Venkatraman, S.; Berry, G. C.; Einaga, Y. Rheological properties of rod-like polymers in solution: 1. Linear and nonlinear steady state behavior. *Macromolecules* 1981, 14, 939–946.
- (40) Berry, G. C.; Metzger-Cotts, P.; Chu, S. G. Thermodynamic and rheological properties of rodlike polymers. *Brit. Polym. J.* **1981**, *13*, 47–54.
- (41) Zero, K. M.; Pecora, R. Rotational and translational diffusion in semidilute solutions of rigid-rod macromolecules. *Macromolecules* **1982**, *15*, 87–93.
- (42) Russo, P. S.; Langley, K. H.; Karasz, F. E. Dynamic light scattering study of semidilute solutions of a stiff chain polymer. *J. Chem. Phys.* **1984**, *80*, 5312–5325.
- (43) Venkatraman, S.; Berry, G. C.; Einaga, Y. Rheological properties of rod-like polymers in solition: 2. Linear and nonlinear transient behavior. *J. Polym. Sci.* **1985**, *23*, 1275–1295.
- (44) Keep, G. T.; Pecora, R. Dynamics of rodlike macromolecules in nondilute solution: Poly(n-alkyl-isocyanates). *Macromolecules* **1988**, *21*, 817–829.
- (45) Kim, S. S.; Han, C. D. Effect of molecular weight on the rheological behavior of thermotropic liquid-crystalline polymers. *Macromolecules* **1993**, *26*, 6633–6642.
- (46) Joly-Duhamel, S.; Hellio, D.; Ajdari, A.; Djabourow, M. All-gelatin networks 2. The mastercurve for elasticity. *Langmuir* **2002**, *18*, 7158–7166.

- (47) Huang, Y. Y.; Ahir, S. V.; Terentjev, E. M. Dispersion rheology of carbon nanotubes in a polymer matrix. *Phys. Rev. B* **2008**, *73*, 125422.
- (48) van Ruymbeke, E.; Nielsen, J.; Hassager, O. Linear and nonlinear viscoelastic properties of bidisperse linear polymers: Mixing law and tube pressure effect. *J. Rheol.* **2010**, *54*, 1155–1172.
- (49) Boudara, V. A. H.; Peterson, J. D.; Leal, L. G.; Read, D. J. Nonlinear rheology of polydisperse blends of entangled linear polymers: Rolie-Double-Polie models. J. Rheol. 2019, 63, 71–91.
- (50) Marrucci, G.; Grizzuti, N. The effect of polydispersity on rotational diffusivity and shear viscosity of rodlike polymers in concentrated solutions. *J. Polym. Sci.* **1983**, *21*, 83–86.
- (51) Marrucci, G.; Grizzuti, N. Predicted effect of polydispersity on rodlike polymer behaviour in concentrated solutions. *J. Non-Newtonian Fluid Mech.* **1984**, *14*, 103–119.
- (52) Doi, M.; Edwards, . F. *The theory of polymer dynamics*; Oxford university Press, New York, 1986.
- (53) Dhont, J. K. G.; Briels, W. J. Viscoelasticity of suspensions of long, rigid rods. *Coll. Surf. A* **2003**, *213*, 131–156.
- (54) Larson, R. G.; Mead, D. W. Toward a quantitive theory of the rheology of concentrated solutions of stiff polymers. *J. Polym. Sci.* **1991**, *29*, 1271–1285.
- (55) Yvon, J. La theorie statistique et l'equation d'état; Herman and Cie, Paris, 1935.
- (56) Born, M.; Green, H. S. A general kinetic theory of liquids I. The molecular distribution functions. *P. Roy. Soc. A Math. Phy.* **1946**, *188*, 10–18.
- (57) Rex, M.; Wensink, H. H.; Loewen, H. Dynamic density functional theory for anisotropic colloidal particles. *Phys. Rev. A* **2007**, *76*, 021403.

- (58) Raveche, H. J.; Green, M. S. On the consistency of the Yvon-Born-Green hierarchy and its truncation. *J. Chem. Phys.* **1969**, *50*, 5334–5336.
- (59) Lang, C.; Kohlbrecher, J.; Porcar, L.; Lettinga, M. P. The connection between biaxial orientation and shear thinning for quasi-ideal rods. *Polymers* **2016**, *8*, 291.
- (60) Forest, M. G.; Wang, Q. Monodomain response of finite-aspect-ratio macromolecules in shear and related linear flows. *Rheol. Acta* **2003**, *42*, 20–46.
- (61) Luria, S. E.; Human, M. L. A nonhereditary, host-induced variation of bacterial viruses.

 J. Bacteriol. 1952, 64, 557–569.
- (62) Bertani, G. The mode of phage liberation by lysogenic escherichia coli. *J. Bacteriol.* **1951**, *62*, 193–300.
- (63) Sambrook, J.; Fritsch, E. F.; T., M. Molecular cloning: a laboratory manual; Cold Spring Harbor Laboratory Press, Cold Spring Harbor, New York, 1989.
- (64) Dogic, Z.; Fraden, S. Ordered phases of filamentous viruses. *Curr. Opin. Colloid In.* **2006**, *11*, 47–55.
- (65) Chen, Z. Y. Nematic ordering in semiflexible polymer chains. *Macromolecules* 1996, 26, 3419–3423.
- (66) Barry, E.; Beller, D.; Dogic, Z. A model liquid crystalline system based on rodlike viruses with variable chirality and persistence length. *Soft Matter* **2009**, *5*, 2563–2570.
- (67) Carreau, P. J. Rheological equations from molecular network theories. J. Rheol. 1972, 16, 99–127.
- (68) Bricker, J. M.; Park, H. O.; Butler, J. E. Rheology of semidilute suspensions of rigid polystyrene ellipsoids at high Peclet numbers. *J. Rheol.* **2008**, *52*, 941–955.

Graphical TOC Entry

